Sensor and Simulation Notes
Note 148
9 May 1972

General Principles for the Design of ATLAS I and II

Part V:

Some Approximate Figures of Merit for Comparing the Waveforms Launched by Imperfect Pulser Arrays onto TEM Transmission Lines

Carl E. Baum
Air Force Weapons Laboratory

Abstract

While detailed calculations of the various effects associated with launching waves on TEM transmission lines from imperfect pulser arrays do not presently exist some of the effects can be noted. Associated with these imperfections in the resulting waveform a few quantitative figures of merit can be defined. Using some very approximate methods (in some cases) rough numbers can be assigned to these figures of merit. In the future more accurate calculations can obtain better numbers for these figures of merit and perhaps suggest a few more appropriate figures of merit.

Sensor and Simulation Notes
Note 148
9 May 1972

General Principles for the Design of ATLAS I and II

Part V:

Some Approximate Figures of Merit for Comparing the Waveforms Launched by Imperfect Pulser Arrays onto TEM Transmission Lines

Carl E. Baum
Air Force Weapons Laboratory

Abstract

While detailed calculations of the various effects associated with launching waves on TEM transmission lines from imperfect pulser arrays do not presently exist some of the effects can be noted. Associated with these imperfections in the resulting waveform a few quantitative figures of merit can be defined. Using some very approximate methods (in some cases) rough numbers can be assigned to these figures of merit. In the future more accurate calculations can obtain better numbers for these figures of merit and perhaps suggest a few more appropriate figures of merit.

I. Introduction

At the present state of the art there are many detailed questions concerned with the design of pulser arrays which have not received much detailed treatment, say in the form of various pertinent electromagnetic boundary value problems. Such pulser arrays are likely approaches to the pulser design for the large EMP simulators for testing aircraft: ATLAS I (a horizontally polarized transmission-line EMP simulator with a trestle test stand) and ATLAS II (a vertically polarized transmission-line EMP simulator with a trestle test stand). The direction of electromagnetic propagation is horizontal in both cases. Parts I through IV of this series (Sensor and Simulation Notes 143 through 146) give more details of the simulator designs.

While there is not yet a large body of solved electromagnetic boundary value problems which analyze the performance of such arrays, still one can use some approximate techniques to estimate the waveforms launched by various arrays onto TEM transmission lines. Even though such techniques may address only some of the array design problems and may not give complete waveforms, still they can be used to make comparisons between one array and another for some of the resulting waveform characteristics.

Too many people seem to think of only peak field or peak field together with 10% to 90% rise rime for EMP waveforms. These are in general quite inadequate by themselves and are often not the important waveform parameters most closely associated with the coupling to the system under test.

The purpose of this note is to define a few parameters of interest to waveforms launched by arrays of capacitive pulse generators onto TEM transmission lines which are assumed terminated in their characteristic impedance or are in effect infinitely long. While cylindrical transmission lines offer some simplification to the arguments and form the basis of most of the calculations, the results should still apply to conical transmission lines (of small divergence angles) with some small modifications.

First some of the important characteristics of waveforms for EMP purposes are discussed. This is followed by a discussion of some figures of merit which can be defined for waveforms resulting from capacitive pulser arrays launching waves onto cylindrical TEM transmission lines. Needless to say such figures of merit are based on this particular field-generation problem and are most appropriate to it; some of these figures of merit may not be appropriate at all for waveforms produced by other means in other geometries. Furthermore since the understanding of such arrays will likely increase as time goes on more figures of merit (and even better ones) will likely be developed.

II. Some Important Characteristics of EMP Waveforms

When considering EMP waveforms, particularly when designing EMP simulators, one should consider how closely the waveform produced approximates some desired or "real" waveform. But what is it that one even asks about waveforms to see how well one approximates another? There are many questions one can ask.

One approach involves direct time domain comparison of the two waveforms basically as two superimposed graphs plotting some component of $\vec{E}$ or $\vec{H}$ as a function of time. What are then seen as obvious differences in amplitude and time characteristics are made a basis of comparison. Such things might include rise time, peak amplitude, pulse width or exponential decay time constant, and perhaps some kind of ripple or noise superimposed on the basic pulse shape (and expressed as a fraction of the peak amplitude or even the instantaneous amplitude of some ideal reference pulse). Certainly this represents a way of making comparisons of "real" waveforms to "ideal" waveforms. However, this method while convenient is not very complete unless one can assume that other waveform features which are not so directly "visible," but which can have significant implications for coupling to a system under test, are in fact not a problem in the case of the particular waveform being considered. Even in the time domain why should one only compare $\vec{E}$ or $\vec{H}$ as a function of time to the ideal waveform. For example one could compare the time derivatives and/or time integrals of these quantities to the "ideal" case; these are just as much time domain waveforms as any others, and rise times, pulse widths, etc. may have somewhat different degrees of approximation between "real" and "ideal" for these derived waveforms.

Note that we have been discussing $\vec{E}$ and $\vec{H}$ types of waveforms so far. This is appropriate for the case of free space (and normal air) because of the simple relations that can be used to obtain the time derivatives of $\vec{D}$ and $\vec{B}$ to give respectively the current and voltage densities.[1] However, for more complicated media such as EMP source regions at least current densities should also be considered.

Another way to look at EMP waveforms is to consider their Fourier transforms and thereby go from time domain to frequency domain. Systems have different sensitivities in different parts of the frequency spectrum. Thus one might determine how closely the magnitudes of the Fourier transforms of "real" and "ideal" waveforms correspond over some band of frequencies of interest to the system response. This band may include many orders of magnitude in frequency. In frequency domain many characteristics of the waveform may become more obvious.

In asking questions about the pertinent features of EMP waveforms for system response one should consider some of the

ways of looking at the interaction of electromagnetic waves with systems. Interaction models involve mathematical concepts and such concepts can be used to formulate questions. At sufficiently high frequencies the interaction of electromagnetic waves with systems is quite often a local phenomenon at some "penetration" into the system. To some extent then concepts of geometrical diffraction theory are applicable implying that high frequency asymptotic forms of waveforms can be useful. At sufficiently low frequencies static or quasi static interaction can be important and the wave equation reduces to the Laplace equation. For this region of frequencies the asymptotic low frequency content of waveforms is useful. At intermediate frequencies important resonance phenomena in systems are observed. From the singularity expansion method[2] these are directly relatable to singularities of the object response in the complex frequency plane. Thus for appropriate intermediate complex frequencies (in a magnitude sense) one can appropriately compare the "real" and "ideal" waveforms not just on the $i\omega$ axis but over portions of the complex frequency plane. It would be somewhat unfortunate to have the Laplace transform of the "real" waveform have a zero where the "ideal" one did not if that complex frequency were close to a pole in the object response.

As one can see there are many ways to evaluate waveforms. One would like to reduce waveform comparisons to a few numbers, but this does not seem reasonable in the most general case. Part of the problem is just knowing the "real" waveform in sufficient detail to ask all these kinds of questions about its characteristics. For a given type of EMP simulator, say a transmission-line EMP simulator driven by a pulser array, one can ask questions about the wave launched by the array onto the transmission line from the viewpoint of those characteristics of the waveform which can be directly linked to features of the array design such as array shape and number of pulsers in the array. The questions one asks are limited by the state of the art in understanding, but that is normally the case. Thus in this note we can formulate a few questions with some techniques for roughly estimating the answers. In some cases the techniques are more useful for relative comparisons between arrays than for determining accurate numbers for the particular waveform characteristics. They can be considered for their conceptual usefulness as well as to get some numbers even if very approximate. However, I expect that future notes will refine these concepts somewhat and develop more accurate numerical estimates.

III. Field Description on a Cylindrical Transmission Line

Two previous notes[3,4] have discussed some of the features of the design of pulser arrays such as can be used on ATLAS I and II. Some effects on the waveform associated with the pulser array parameters were discussed in these previous notes, and some techniques for improving the waveform with respect to these effects were also discussed. In this note some parameters are associated with the corresponding waveform features discussed before.

Let us first consider some of the early time effects. For this purpose let the capacitance of the pulse generators in the individual array elements be sufficiently large that the RC decay time of the array driving the terminated transmission line is large compared to times of interest. This allows one to consider early time effects as the deviation of the waveform from a step function. Early time (high frequency) and late time (low frequency) characteristics are then approximately separated. Note that this separation may not be very accurate if the array size is made large enough that transit times across the array are of the order of or larger than the effective pulse width (or RC decay time).

Look at the effect of the finite array size. Referring to figure 1 we have an array driving a cylindrical transmission line. The transmission line is shown as two parallel conducting sheets, one at least being of finite width, but other cross section geometries are possible. The pulser array is shown as planar and sloped at some angle ξ with respect to the direction of propagation on the transmission line. Other array geometries, including non planar, are also possible. For our initial consideration the source electric field distribution is assumed continuous over the finite area of the array thereby implying a large number of array elements. Thus one can think of the pulser array as a source surface S_S with a source electric field $\vec{E}_S(\vec{r}_S,t)$ tangential to this surface and distributed over it in some prescribed manner. $\vec{r}_S$ gives the coordinates on S_S.

Besides the source surface we need an effective aperture plane A which is perpendicular to the direction of propagation. Let the electric field on this surface be $\vec{E}_A(x,y,t)$. The basic procedure is then to estimate $\vec{E}_A$, given $\vec{E}_S$ and then use $\vec{E}_A$ to estimate the TEM mode on the cylindrical transmission line. The aperture plane A is placed as near as possible to S_S without intersecting it. This choice is made so as to minimize the amount of transmission line conductors for negative z since the modal expansion is used for positive z for the cylindrical transmission line and such conductors for negative z complicate matters. For our coordinate system note that A is the x,y plane and the TEM mode launched on the cylindrical transmission line propagates in the positive z direction.

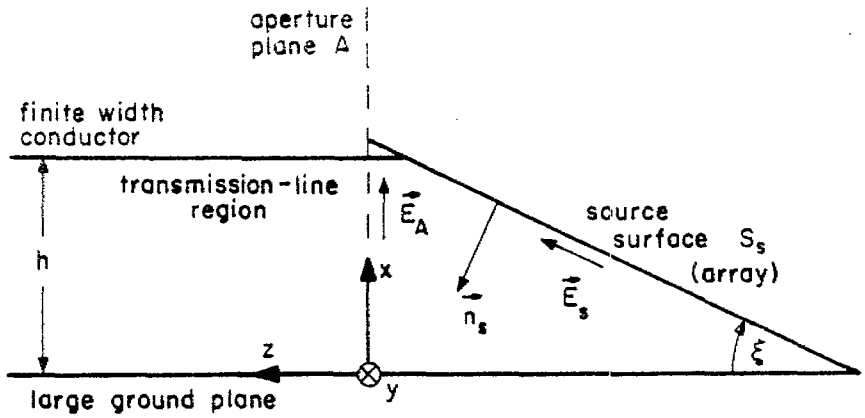

A. SIDE VIEW

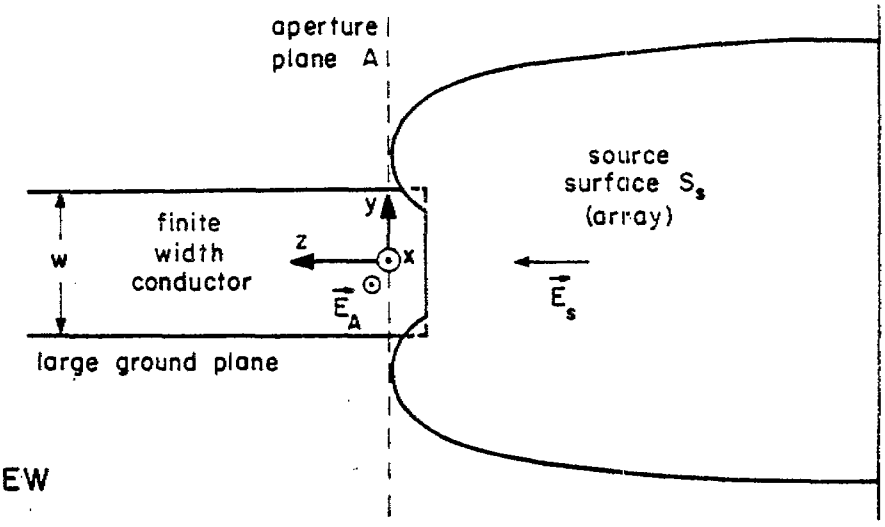

B. TOP VIEW

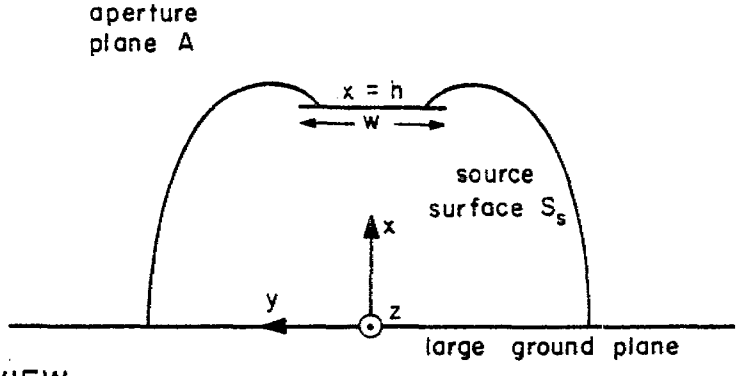

C. FRONT VIEW

FIGURE I. FINITE SIZE SOURCE ARRAY DRIVING CYLINDRICAL TRANSMISSION LINE

While a detailed solution of an appropriate boundary value problem (such as for the geometry in figure 1) is beyond the scope of this note, still one can learn something of the form of the solution. For this purpose we have

$$c = \frac{1}{\sqrt{\mu_o \varepsilon_o}}, \quad Z_o = \sqrt{\frac{\mu_o}{\varepsilon_o}}$$
$$\gamma = \frac{s}{c} \tag{1}$$

where we have the permeability μ_o, permittivity ε_o, and Laplace transform variable s (with respect to time). Using a tilde ~ to denote the Laplace transform we can expand the electric field for $z > 0$ (the transmission line region) in the general form[5]

$$\tilde{\vec{E}}(\vec{r},s) = E_o \sum_\alpha \tilde{a}_\alpha(s) e^{-\gamma_\alpha z} \tilde{\vec{g}}_\alpha(x,y,s) + \tilde{\vec{E}}_R(\vec{r},s) \tag{2}$$

where α is a mode index, $\tilde{\vec{g}}_\alpha(x,y,s)$ is the mode distribution (with possibly x, y, and z components), and $\tilde{a}_\alpha(s)$ is the mode coefficient. These latter two may be functions of the complex frequency s. The z variation is contained in the exponentials with propagation constants γ_α which are functions of s (or γ). Note that while a discrete spectrum is indicated by the sum over α in equation 2 we can still allow this sum to also include an integral over α for part of its range to give a continuous spectrum in γ_α if this is needed. The additional term $\tilde{\vec{E}}_R$ has a continuous spectrum and is termed the radiation field. Note that by Laplace transforming this term over the z axis ($0 \leq z \leq \infty$) and then inverse transforming we have an integral over γ_α effectively, so we can let the sum be over discrete γ_α.

The lowest order mode is the TEM mode which for convenience we designate by $\alpha = 0$ for which we have

$$\tilde{\vec{g}}_{TEM}(x,y,s) \equiv \tilde{\vec{g}}_o(x,y,s) \equiv \vec{g}_o(x,y)$$
$$\gamma_{TEM} \equiv \gamma_o \equiv \gamma \tag{3}$$

since it is well known that the TEM mode propagates at speed c with a frequency independent mode function. Note that $\vec{g}_o$ has no z component and that it can be expressed as a purely real valued vector function of x and y.

There are various cross section geometries of cylindrical transmission lines consisting of two or more separate perfect conductors in a uniform, isotropic, lossless, and frequency independent medium that one might consider. An important example is the one consisting of two symmetrically positioned perfectly conducting parallel plates, or equivalently a single finite width perfectly conducting plate parallel to an infinitely wide one as shown in figure 1. This example has been studied in previous notes[6,7] and has been an important example with a significant influence on the design of ALECS, ARES, and now the simulators ATLAS I and II under design.

Understanding this TEM mode can give us tools for characterizing the waveform launched on a cylindrical transmission line by imperfect pulser arrays. At sufficiently low frequencies (wavelengths much larger than h and w) the fields at large z ($z >> h,w$) in the immediate vicinity of the transmission line are given by the TEM mode. Except near the source the fields on the transmission line reduce to a circuit problem using transmission line theory with the TEM mode.

The problem of concern is what happens at high frequencies with wavelengths of the order of or less than the cross section dimensions of the transmission line. It is well known that the TEM mode propagates at speed c with no loss at all frequencies. Given the linear nature of this problem the TEM mode can be added in any proportion to any solution of Maxwell's equations matching the boundary conditions on the transmission line conductors. To this extent (at least) the TEM mode can be considered independent of the rest of the fields on the cylindrical transmission line.

Now in the TEM mode we have the well known property that

$$\tilde{\vec{E}}_{TEM}(\vec{r},s) = E_o \tilde{a}_o(s) e^{-\gamma z} \vec{g}_o(x,y)$$

$$\tilde{\vec{H}}_{TEM}(\vec{r},s) = \frac{1}{Z_o} \vec{e}_z \times \tilde{\vec{E}}_{TEM} = \frac{E_o}{Z_o} \tilde{a}_o(s) e^{-\gamma z} \vec{h}_o(x,y) \qquad (4)$$

$$\vec{h}_o(x,y) = \vec{e}_z \times \vec{g}_o(x,y) \ , \quad \vec{g}_o(x,y) = -\vec{e}_z \times \vec{h}_o(x,y)$$

where $\vec{e}$ with a subscript denotes a unit vector for the coordinate indicated. In a form similar to equation 2 the magnetic field is expanded as

$$\tilde{\vec{H}}(\vec{r},s) = \frac{E_o}{Z_o} \sum_{\alpha} \tilde{a}_\alpha(s) e^{-\gamma_\alpha z} \tilde{\vec{h}}_\alpha(x,y,s) + \tilde{\vec{H}}_R(\vec{r},s) \qquad (5)$$

The individual terms in the modal expansion and the "radiation" term for each satisfy Maxwell's equations without sources. Our sources are taken to be in $z < 0$ and so are not needed in this expansion. Sometimes it is convenient to use the components tangential to the x,y plane defined by

$$\tilde{\vec{g}}_{t_\alpha}(x,y,s) = [\vec{\vec{I}} - \vec{e}_z\vec{e}_z] \cdot \tilde{\vec{g}}_\alpha(x,y,s)$$

$$\tilde{\vec{h}}_{t_\alpha}(x,y,s) = [\vec{\vec{I}} - \vec{e}_z\vec{e}_z] \cdot \tilde{\vec{h}}_\alpha(x,y,s) \tag{6}$$

where the identity dyadic is defined by

$$\vec{\vec{I}} \equiv \vec{e}_x\vec{e}_x + \vec{e}_y\vec{e}_y + \vec{e}_z\vec{e}_z \tag{7}$$

Using the Lorentz reciprocity theorem

$$\int_S [\tilde{\vec{E}}_1 \times \tilde{\vec{H}}_2 - \tilde{\vec{E}}_2 \times \tilde{\vec{H}}_1] \cdot \vec{n}dS = \int_V \tilde{\vec{J}}_1 \cdot \tilde{\vec{E}}_2 dV \tag{8}$$

where $\vec{n}$ is the outward pointing unit vector normal on S, the closed surface bounding the volume V, and $\tilde{\vec{E}}_1$, $\tilde{\vec{H}}_1$ are a solution of Maxwell's equations for source current density $\tilde{\vec{J}}_1$, and $\tilde{\vec{E}}_2$, $\tilde{\vec{H}}_2$ are a solution of Maxwell's equations without a source term. Setting the source current density to zero gives

$$\int_S [\tilde{\vec{E}}_1 \times \tilde{\vec{H}}_2 - \tilde{\vec{E}}_2 \times \tilde{\vec{H}}_1] \cdot \vec{n}dS = 0 \tag{9}$$

which relates two solutions of Maxwell's equations when no sources are included in V.

Now let the terms in equation 9 be separate terms from the field expansions in equations 2 and 5 since each pair of such terms separately solves the sourceless Maxwell equations. Thus we can write

$$\int_S e^{-\gamma_\alpha z - \gamma_\beta z} [\tilde{\vec{g}}_\alpha(x,y,s) \times \tilde{\vec{h}}_\beta(x,y,s) - \tilde{\vec{e}}_\beta(x,y,s) \times \tilde{\vec{h}}_\alpha(x,y,s)] \cdot \vec{n}dS = 0 \tag{10}$$

Next let S be two infinite planes of constant $z > 0$, say z_1 and z_2. Call these surfaces S_1 and S_2 respectively. Keeping z_1 fixed and varying z_2 the change in the exponential on the surface z_2 requires that the integral over S_1 and S_2 be separately zero. The integral at infinity (large $\sqrt{x^2 + y^2}$) is made zero by imposing a radiation condition at infinity on the modes; essentially this is the requirement for such modes to be considered guided or bound to the transmission line in our case. Note that the TEM mode falls off like a static line dipole since we constrain no net current in the conductors at any cross section for this mode; the TEM mode fields then fall off like $[x^2 + y^2]^{-1}$ and as long as the other modes or radiation fields are bounded at ∞ then this integral at infinity is zero. We then have for any cross section plane such as A the result

$$\int_{S_1} [\tilde{\vec{g}}_\alpha(x,y,s) \times \tilde{\vec{h}}_\beta(x,y,s) - \tilde{\vec{g}}_\beta(x,y,s) \times \tilde{\vec{h}}_\alpha(x,y,s)] \cdot \vec{e}_z dS = 0 \qquad (11)$$

This can also be written in terms of the transverse parts since the z components give no contribution as

$$\int_{S_1} [\tilde{\vec{g}}_{t_\alpha}(x,y,s) \times \tilde{\vec{h}}_{t_\beta}(x,y,s) - \tilde{\vec{g}}_{t_\beta}(x,y,s) \times \tilde{\vec{h}}_{t_\alpha}(x,y,s)] \cdot \vec{e}_z dS = 0 \qquad (12)$$

Now reverse the direction of propagation of one of the sourceless modes, say the α one. This reverses the sign of γ_α and the sign of the transverse magnetic field components. Using this in equations 10 and 11 reverses the sign between the cross products and this gives for comparison to equation 12 the results

$$\int_{S_1} [\tilde{\vec{g}}_{t_\alpha}(x,y,s) \times \tilde{\vec{h}}_{t_\beta}(x,y,s) + \tilde{\vec{g}}_{t_\beta}(x,y,s) \times \tilde{\vec{h}}_{t_\alpha}(x,y,s)] \cdot \vec{e}_z dS = 0 \qquad (13)$$

Combining equations 12 and 13 gives

$$\int_{S_1} [\tilde{\vec{g}}_{t_\alpha}(x,y,s) \times \tilde{\vec{h}}_{t_\beta}(x,y,s)] \cdot \vec{e}_z dS$$

$$= \int_{S_1} [\tilde{\vec{g}}_\alpha(x,y,s) \times \tilde{\vec{h}}_\beta(x,y,s)] \cdot \vec{e}_z dS = 0 \qquad (14)$$

$$\int_{S_1} [\tilde{\vec{g}}_{t_\beta}(x,y,s) \times \tilde{\vec{h}}_{t_\alpha}(x,y,s)] \cdot \vec{e}_z dS$$

$$= \int_{S_1} [\tilde{\vec{g}}_{\beta}(x,y,s) \times \tilde{\vec{h}}_{\alpha}(x,y,s)] \cdot \vec{e}_z dS = 0$$

where the cross products can also be reversed to put the magnetic mode first. This general result expresses the mode orthogonality for general waveguiding structures involving only reciprocal media. This is the case for cylindrical TEM transmission lines involving only uniform media surrounding perfect conductors (or even imperfect conductors). Note that the orthogonality also applies for modes traveling in opposite directions unless $\gamma_\alpha = \gamma_\beta$ in which case these two degenerate modes can be made orthogonal by a common procedure; if it is the same mode (only one independent mode not counting reversal of propagation direction) then of course the mode is not orthogonal to itself. Note that the orthogonality also applies between a mode and the "radiation field."

So far we have been considering general properties of cylindrical waveguiding systems. However, TEM modes on cylindrical transmission lines have rather special properties. From the free space wave equation (transformed) we have for any mode propagating in the z direction with propagation constant γ the result

$$\vec{0} = [\nabla^2 - \gamma^2]\tilde{\vec{E}}(x,y,s)e^{-\gamma z}$$

$$= e^{-\gamma z}\nabla^2\tilde{\vec{E}}(x,y,s) \qquad (15)$$

so that the individual components of $\tilde{\vec{E}}$ satisfy the Laplace equation. In particular we have

$$0 = \nabla^2\tilde{E}_z(x,y,s) \qquad (16)$$

Now $\tilde{E}_z$ must be zero on the conducting boundaries of our cylindrical transmission line and of course we require it to be zero at infinity. The only function satisfying the Laplace equation with zero values on the boundaries is identically zero. Thus $\tilde{\vec{E}}$ must have no z component and a similar argument applies for $\tilde{\vec{H}}$. Thus

$$\gamma_\alpha \neq \gamma \quad \text{for} \quad \alpha \neq 0 \qquad (17)$$

and any waves traveling with speed c in the z direction must be TEM. Thus there can also be no modal degeneracy between TEM modes and non TEM modes or between TEM modes and the radiation fields. Degeneracy of a TEM mode can only apply with respect to another TEM mode.

From equations 4 and 14 let one mode be the TEM mode and the other some other mode or the radiation field giving

$$0 = \int_{S_1} [\tilde{\vec{g}}_\alpha(x,y,s) \times \vec{h}_o(x,y)] \cdot \vec{e}_z dS$$

$$= \int_{S_1} [\tilde{\vec{g}}_\alpha(x,y,s) \times [\vec{e}_z \times \vec{g}_o(x,y)] \cdot \vec{e}_z dS$$

$$= \int_{S_1} [\vec{e}_z [\tilde{\vec{g}}_\alpha(x,y,s) \cdot \vec{g}_o(x,y)] - \vec{g}_o(x,y) [\tilde{\vec{g}}_\alpha(x,y,s) \cdot \vec{e}_z]] \cdot \vec{e}_z dS$$

$$= \int_{S_1} \tilde{\vec{g}}_\alpha(x,y,s) \cdot \vec{g}_o(x,y) dS \qquad (18)$$

since $\vec{g}_o$ is perpendicular to $\vec{e}_z$. This gives the important and useful result that the TEM mode is orthogonal to any non TEM mode and the radiation field in a dot product integral sense, a more common way of thinking of orthogonal functions. Carrying through the same steps starting with $\tilde{\vec{h}}_\alpha$ and $\vec{g}_o$ we also have

$$0 = \int_{S_1} \tilde{\vec{h}}_\alpha(x,y,s) \cdot \vec{h}_o(x,y) dS \qquad (19)$$

so that this orthogonality applies to both electric and magnetic fields. While the integrals apply on an arbitrary cross-section plane S_1, this orthogonality will be typically applied to the aperture plane A.

With the orthogonality relationships one can calculate the coefficients in the modal expansion using equations 2 and 14 as

$$a_\alpha(s) = \frac{\frac{1}{E_o} \int_A [\tilde{\vec{E}}_A(x,y,s) \times \tilde{\vec{h}}_\alpha(x,y,s)] \cdot \vec{e}_z dS}{\int_A [\tilde{\vec{g}}_\alpha(x,y,s) \times \tilde{\vec{h}}_\alpha(x,y,s)] \cdot \vec{e}_z dS} \qquad (20)$$

where the aperture electric field is

$$\tilde{\vec{E}}_A(x,y,s) \equiv \tilde{\vec{E}}(\vec{r},s)\big|_{z=o} \tag{21}$$

In terms of the aperture magnetic field we have

$$\tilde{a}_\alpha(s) = \frac{\frac{Z_o}{E_o}\int_A [\tilde{\vec{H}}_A(x,y,s) \times \tilde{\vec{g}}_\alpha(x,y,s)] \cdot \vec{e}_z dS}{\int_A [\vec{h}_\alpha(x,y,s) \times \vec{g}_\alpha(x,y,s)] \cdot \vec{e}_z dS} \tag{22}$$

$$\tilde{\vec{H}}_A(x,y,s) \equiv \tilde{\vec{H}}(\vec{r},s)\big|_{z=o}$$

For the case of the TEM mode the expression for the mode coefficient can be written as

$$\tilde{a}_o(s) = \frac{\frac{1}{E_o}\int_A \tilde{\vec{E}}_A(x,y,s) \cdot \vec{g}_o(x,y)\,dS}{\int_A \vec{g}_o(x,y) \cdot \vec{g}_o(x,y)\,dS}$$

$$= \frac{\frac{Z_o}{E_o}\int_A \tilde{\vec{H}}_A(x,y,s) \cdot \vec{h}_o(x,y)\,dS}{\int_A \vec{h}_o(x,y) \cdot \vec{h}_o(x,y)\,dS} \tag{23}$$

Since $\vec{g}_o$ and $\vec{h}_o$ are simply related from equations 4 other forms can also be readily derived. Since the TEM mode distribution is independent of s then the coefficient can be written in time domain form as

$$\alpha_o(t) = \frac{\frac{1}{E_o}\int_A \vec{E}_A(x,y,t) \cdot \vec{g}_o(x,y)\,dS}{\int_A \vec{g}_o(x,y) \cdot \vec{g}_o(x,y)\,dS}$$

$$= \frac{\frac{Z_o}{E_o}\int_A \vec{H}_A(x,y,t) \cdot \vec{h}_o(x,y)\,dS}{\int_A \vec{h}_o(x,y) \cdot \vec{h}_o(x,y)\,dS} \tag{24}$$

With these expressions we can calculate the frequency and/or time domain characteristics of the TEM mode waveform in terms of the field distribution on the aperture plane A. By direct extension these coefficients can also be found in terms of the fields at any other cross section plane such as S_1.

The orthogonality result for the TEM mode leading to the TEM mode waveform in equation 24 forms the basis of some of the figure-of-merit definitions in the next section. Based on this integral some very approximate procedures for estimating TEM waveforms can be developed. As one moves to larger values of z one generally expects the TEM mode to be the dominant part of the fields. The higher order modes (non TEM) will likely tend to attenuate with distance for open structures since these modes in part correspond to multiple reflections in parallel plate structures which tend to eventually scatter out of the transmission line structure. In closed lossless TEM transmission lines (such as a coaxial transmission line) such higher order modes are not attenuated unless the frequency is below some cutoff frequency. The detailed characteristics of higher order modes in parallel plate transmission lines are not well understood at present except for being orthogonal to the TEM mode. In any event we take for our definition of an "average" waveform on the transmission line the TEM mode; from equation 24 the TEM waveform at plane S_1 can obviously be regarded as such an average. As one samples across a cross section of the transmission line different time domain waveforms may be observed. However, it would be useful to reduce such observations to one waveform to make the waveform analysis simpler. At some future time it may be desirable to consider some of the higher order modes to further refine the quantitative consideration of waveform quality. In this note waveform quality is discussed in terms of the TEM mode.

IV. Definition of Some Figures of Merit for Pulser Arrays

Now let us obtain some approximate waveform characteristics for the TEM mode launched on a cylindrical transmission line by a finite size source array. For this purpose it is convenient to concentrate on the time domain form of $\alpha_o(t)$ as given by equation 24 in terms of the aperture electric field $\vec{E}_A(t)$. The waveform characteristics discussed in this section are summarized in figure 2.

First let us consider some of the early-time characteristics of the waveform. For this purpose assume that we have a source with zero impedance at low frequencies (infinite capacitance) so that the late time characteristics of $\alpha_o(t)$ are those of a step function. This is later modified to include the RC decay characteristics. For normalization purposes then choose E_o such that $\alpha_o(t)$ tends to 1.0 at late times for zero internal source impedance at low frequencies. The equivalent source generator is a step function which is distributed at many positions over the array. Letting V_o be the late time step function voltage we have for $z > 0$

$$V_o = -\int_o^h E_x\Big|_{\substack{y=o \\ t \text{ large}}} dx = -E_o \int_o^h g_{x_o}\Big|_{y=o} dx$$

$$= -E_o \int_C \vec{g}_o(x,y) \cdot d\vec{\ell} \tag{25}$$

where C is a path with differential line element $d\vec{\ell}$ from the plate on $x = 0$ to the finite width plate on $x = h$. Note that the TEM mode $\vec{g}_o$ can be expressed as

$$\vec{g}_o(x,y) = -\nabla\Phi(x,y) \tag{26}$$

where $\Phi(x,y)$ is a scalar potential function with

$$\Phi(h,y)\Big|_{|y| \le \frac{w}{2}} - \Phi(0,y) = \frac{V_o}{E_o} \tag{27}$$

where the two values of y need not be the same. As long as the ends of C are fixed on the two plates then the line integral in equation 25 is independent of the path. From equation 27 one can appropriately choose E_o such that at late times the TEM part of $\vec{E}_A/E_o$ is just $\vec{g}_o$, automatically making $\alpha_o(t) \to 1$ at late times. For convenience with this normalization define

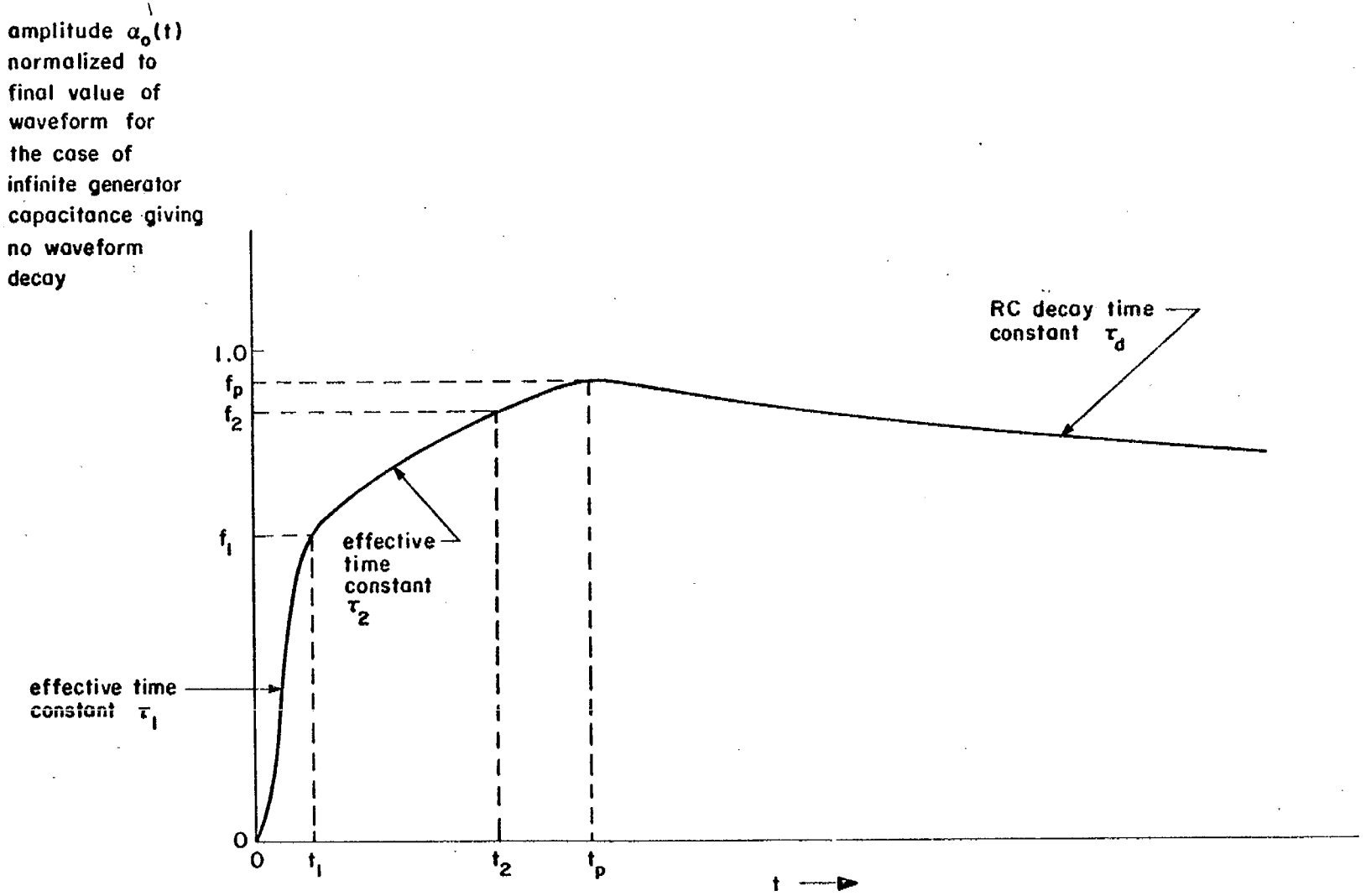

FIGURE 2. NOMINAL WAVEFORM FOR TEM MODE ON CYLINDRICAL TRANSMISSION LINE

$$\vec{g}_A(x,y,t) \equiv \frac{\vec{E}_A(x,y,t)}{E_o} \tag{28}$$

as our normalized electric field at the aperture plane. The TEM waveform can then be written as

$$\alpha_o(t) = \frac{\int_A \vec{g}_A(x,y,t) \cdot \vec{g}_o(x,y)\,dS}{\int_A \vec{g}_o(x,y) \cdot \vec{g}_o(x,y)\,dS} \tag{29}$$

As a first early time consideration let the array be represented as a continuously distributed source surface S_s as shown in figure 1. Let the electric field on the source surface be prescribed as a step function in retarded time with respect to z so that it has the form

$$\vec{E}_s(\vec{r}_s,t) = \vec{E}_{s_o}(x_s,y_s)\,u\left(t - \frac{z_s}{c}\right) \tag{30}$$

where

$$\vec{r}_s = x_s\vec{e}_x + y_s\vec{e}_y + z_s\vec{e}_z \tag{31}$$

gives the coordinates on S_s and $\vec{E}_s$ is the tangential components of the electric field on S_s. Let $\vec{n}_s$ be the surface normal for S_s as indicated in figure 1.

As in figure 1C the finite size source surface can be projected onto the aperture plane; call this portion of the aperture plane A_s. From geometrical diffraction theory the electric fields on A at t = 0+ are zero on A - A_s and in general non-zero on A_s given by

$$[\vec{\vec{I}} - \vec{n}_s(x,y)\vec{n}_s(x,y)] \cdot \vec{E}_A(x,y,0+) = \vec{E}_{s_o}(x,y) \tag{32}$$

with x_s, y_s being the same as x,y for this calculation. In normalized form this is

$$[\vec{\vec{I}} - \vec{n}_s(x,y)\vec{n}_s(x,y)] \cdot \vec{g}_A(x,y,0+) = \frac{\vec{E}_{s_o}(x,y)}{E_o} \tag{33}$$

We can also write this as

$$\vec{n}_s \times \vec{g}_A(x,y,0+) = \vec{n}_s \times \frac{\vec{E}_{s_o}(x,y)}{E_o} \tag{34}$$

Since $\vec{g}_A(x,y,0+)$ has only x and y components (transverse to the direction of propagation in the high-frequency limit) we can write

$$-\vec{e}_z \cdot \vec{n}_s(x,y)\vec{n}_s(x,y) \cdot \vec{g}_A(x,y,0+) = \vec{e}_z \cdot \frac{\vec{E}_{s_o}(x,y)}{E_o} \tag{35}$$

so that equation 33 can be rewritten as

$$\vec{g}_A(x,y,0+) = \left[\vec{\vec{I}} - \frac{\vec{n}_s(x,y)\vec{e}_z}{\vec{n}_s(x,y) \cdot \vec{e}_z}\right] \cdot \frac{\vec{E}_{s_o}(x,y)}{E_o} \tag{36}$$

Note that if $\vec{n}_s \cdot \vec{e}_z$ becomes zero this is not a problem if $\vec{E}_{s_o}$ is also made zero for such regions of S_s.

For the special case that $\vec{n}_s$ has no y component because S_s is described as a function of x and z only, then the results simplify somewhat. In particular if the source surface is also flat and inclined at an angle ξ (in the x, z plane) with respect to the y, z plane then

$$\vec{n}_s \cdot \vec{e}_x = -\cos(\xi) \ , \quad \vec{n}_s \cdot \vec{e}_y = 0 \ , \quad \vec{n}_s \cdot \vec{e}_z = \sin(\xi)$$

$$\vec{e}_z \cdot \vec{E}_{s_o}(x,y) = \cos(\xi)E'_{s_o}(x,y) \ , \quad \vec{e}_x \cdot \vec{E}_{s_o}(x,y) = \sin(\xi)E'_{s_o}(x,y) \tag{37}$$

where E'_{s_o} is the component of $\vec{E}_{s_o}$ parallel to the x, z plane (or perpendicular to $\vec{e}_y$) and it is taken positive in the direction of increasing x. In this case equation 36 reduces to

$$g_{A_x}(x,y,0+) = \frac{1}{\sin(\xi)} \frac{E'_{s_o}(x,y)}{E_o}$$

$$g_{A_y}(x,y,0+) = \frac{E_{s_{o_y}}(x,y)}{E_o} \tag{38}$$

For such flat source surfaces it is then rather simple to relate the initial aperture electric field to the initial source electric field which is based on the distribution and voltages of the generators (to obtain volts/meter) on the source surface.

Now define one figure of merit for such a source array driving a cylindrical TEM transmission line as

$$f_1 \equiv \alpha_1(0+) = \frac{\int_A \vec{g}_A(x,y,0+) \cdot \vec{g}_o(x,y)\,dS}{\int_A \vec{g}_o(x,y) \cdot \vec{g}_o(x,y)\,dS} = \frac{\int_{A_s} \vec{g}_A(x,y,0+) \cdot \vec{g}_o(x,y)\,dS}{\int_A \vec{g}_o(x,y) \cdot \vec{g}_o(x,y)\,dS} \tag{39}$$

This number represents the fractional initial rise of the TEM waveform. For ordinary capacitive generators in an array for which A_s does not completely cover the area for which $\vec{g}_o(x,y) \neq \vec{0}$ this number is typically less than 1.0. Including extra voltage on each generator in a manner which applies only to early times would correspond to increasing $\vec{g}_A(x,y,0+)$ and thereby raise f_1 by compensating for the non use of the portion of the aperture surface $A - A_s$. However, this would require additional features in each generator or special generators distributed among the other generators on the source surface. In any event f_1 is one number for comparing array designs to see which puts out the better waveform.

Having formulated the integral for $\alpha_o(t)$ there is still the problem of calculating waveforms because of the complexity of the fields on A. We need to estimate $\vec{g}_A(x,y,t)$ in order to compute the integral. The early time ($t = 0+$) form is obtained by a geometrical diffraction method as discussed above. One way to try to calculate $\vec{g}_A$ for longer times is to use more terms in a geometrical diffraction theory expansion including the arrival time of such terms on the $A - A_s$ portion of the aperture plane. Note that as the position of A is moved to larger z values ($z > 0$) the initial fields on A_s (at $t = (z/c)+$) remain the same giving the same value for f_1. The fields arrive on portions of $A - A_s$ at earlier retarded times as A is moved to larger z, but the initial field amplitudes reaching the same portions of $A - A_s$ become smaller, or stated better the coefficients of the early time asymptotic forms of the fields reaching $A - A_s$ become smaller. This is consistent with the fact that $\alpha_o(t)$ must be independent of z_1 for $z_1 \geq 0$ as the new position of A since the TEM mode only has a retarded time variation with z. Turning on portions of $A - A_s$ faster is compensated to some extent by smaller $\vec{g}_A$ magnitudes there at early times.

The geometrical diffraction method does not in general apply at all for late times. Furthermore it would be desirable to have some simpler method to estimate waveforms, at least for

relative comparisons among various array designs. This simple method might be termed a sequential turn on method. In this method one approximates $\vec{g}_A$ as

$$\vec{g}_A^*(x,y,t) \equiv \vec{g}_o(x,y)\,u(t_A(x,y)) \tag{40}$$

where $t_A(x,y) = 0$ at the first time any fields reach the position x, y on A. The asterisk superscript indicates a quantity replaced by the value calculated by the sequential turn on method. Thus for f_1 we would estimate

$$f_1^* = \frac{\int_A \vec{g}_A^*(x,y,0+) \cdot \vec{g}_o(x,y)\,dS}{\int_A \vec{g}_o(x,y) \cdot \vec{g}_o(x,y)\,dS} = \frac{\int_{A_s} \vec{g}_o(x,y) \cdot \vec{g}_o(x,y)\,dS}{\int_A \vec{g}_o(x,y) \cdot \vec{g}_o(x,y)\,dS} \tag{41}$$

Note that f_1^*, while not in general the same as f_1, still is invariant with respect to our choice of $z = z_1 \geq 0$ as the position of A in case we were to move A to some other z. However for later times the choice of the $z = z_1$ position for A does make a difference. In particular as z_1 is increased the subsequent rise of the waveform beyond f_1^* becomes faster. Thus in comparing two array designs for the rise beyond f_1 using the sequential turn on method one should be consistent in the choice of z_1, the position of A. Since the idea is to point out differences between different array designs (and not to mask these differences) then the position of A should be chosen as close to the array as possible. Of course if a sloped array extends past its intersection with the transmission line conductors in the direction of positive z (as shown in figure 1) then the plane A should be taken before the end of those conductors but as close as possible. For comparison to arrays which do not extend out as far but are driving the same geometry of transmission line the plane A should be chosen at the same common position on the transmission line at a place which makes A clear of all the array shapes being considered.

One interesting type of array is the curvilinear array discussed in reference 3. This also applies to sloped arrays discussed in reference 4. A curvilinear array is one which has the source field (in the continuous approximation) specified as

$$\vec{E}_s(\vec{r}_s,t) = \vec{E}_{s_o}(x_s,y_s)\,u\left(t - \frac{z_s}{c}\right)$$

$$\frac{\vec{E}_{s_o}(x,y)}{E_o} = [\vec{\vec{I}} - \vec{n}_s(x,y)\vec{n}_s(x,y)] \cdot \vec{g}_A(x,y,0+) \tag{42}$$

$$\vec{g}_A(x,y,0+) = \begin{cases} \vec{g}_o(x,y) \text{ for } x,y \in A_s \\ 0 \text{ for } x,y \notin A_s \end{cases}$$

In other words the source electric field is specified to be the projection of the TEM electric field on the source surface where projection is done in the z direction along lines of constant x and y and the components of $\vec{g}_o(x,y)$ tangential to S_s define the normalized source electric field there. Note that S_s is still a finite surface so even a curvilinear array in this sense is not perfect. However, it does give the special result

$$\vec{g}_A^*(x,y,0+) = \vec{g}_A(x,y,0+)$$

$$f_1^* = f_1 \tag{43}$$

Thus for the initial rise characteristics of an array the geometrical diffraction method and sequential turn on method become the same. However, this early time result does not carry over into later times even for curvilinear arrays.

Curvilinear arrays have other interesting properties. If we define a complex potential function

$$w(\zeta) = u(x,y) + iv(x,y)$$

$$\zeta = x + iy \tag{44}$$

such that the electric potential function, $u(x,y)$, is a constant u_1 on one conductor and a different constant u_2 on the other conductor then we have the interesting result

$$\vec{g}_o(x,y) = \nabla u(x,y)$$

$$\vec{h}_o(x,y) = \nabla v(x,y) \tag{45}$$

where $v(x,y)$ is the magnetic potential function or stream function. This allows one to define a complex mode function as

$$\vec{W}(x,y) = \vec{g}_o(x,y) + i\vec{h}_o(x,y) = \nabla w(\zeta) \tag{46}$$

This can be rewritten using complex mode functions and the Cauchy-Riemann conditions as

$$\begin{aligned} g_o(\zeta) &= g_{o_x}(x,y) + ig_{o_y}(x,y) \\ h_o(\zeta) &= h_{o_x}(x,y) + ih_{o_y}(x,y) \\ g_{o_x}(x,y) &= h_{o_y}(x,y) \ , \quad g_{o_y}(x,y) = -h_{o_x}(x,y) \\ h_o(\zeta) &= ig_o(\zeta) \end{aligned} \tag{47}$$

giving

$$g_o(\zeta) = -ih_o(\zeta) = \frac{\partial w(\zeta)}{\partial \zeta} \tag{48}$$

If a curvilinear array is made such that the projection of S_S on A to give A_S results in a surface A_S bounded by the transmission line conductors ($u = u_1, u_2$) and two stream function values (say $v = v_1, v_2$ or some other even number of values) then at low frequencies current is continuous through the array as discussed in reference 3. Current paths are continuous along electric field lines so as not to be interrupted in traveling between the two transmission line conductors. Of course non curvilinear arrays can also be constructed with this property.

One can picture a curvilinear array by plotting contours of fixed values of the u and v functions on the aperture plane for equal changes in u and equal changes in v, although the changes in u and v between their respective contours need not be the same. The curvilinear rectangles so formed on A_S define the location of pulsers, each of equal voltage and equal low frequency impedance (capacitance in the usual case). This curvilinear pattern is projected from A_S onto S_S keeping x and y fixed in the transformation. On S_S the generators establish the potential between the projected contours of u. If one looks perpendicular to S_S (along $\hat{n}_S$) the curvilinear pattern is not necessarily rectangular unless $\hat{n}_S = \pm\hat{e}_z$.

Note that for the case that the early time $\vec{E}_s$ as projected on A_s is just $\vec{g}_o$ then the integral for f_1 (or $\alpha_o(0+)$) is an integral of the square of the local electric field. Since the area of a curvilinear rectangle is proportional to $|\nabla u|^{-1} |\nabla v|^{-1}$ it is proportional to $|\vec{g}_o(x,y)|^{-2}$ or $|\vec{h}_o(x,y)|^{-2}$. The power in each curvilinear rectangle where $\vec{g}_o$ is the normalized electric field is then the same. Thus the power passing through A at $t = 0+$ is f_1 relative to the late time power for fixed voltage step V_o on the array. Note that f_1^2 is the power in the TEM mode at the surface A at $t = 0+$. The power at A in the higher order modes and radiation field at $t = 0+$ is then $f_1 - f_1^2$ or $f_1(1 - f_1)$ which is ideally a small number.

Now if the curvilinear array S_s has the boundaries of its projection A_s defined by the two (or more) conductors with potential function contours u_1, u_2 and by two stream function contours v_1, v_2 and if Δv is the change of stream function around one of the conductors with $v_2 > v_1$ and v continuous between v_1 and v_2 then the early time TEM mode fraction is just

$$f_1 = \frac{v_2 - v_1}{\Delta v} \tag{49}$$

A simple way of viewing this result is to let the curvilinear rectangles be the differential area elements but observe that $\vec{g}_o \cdot \vec{g}_o$ is inversely proportional to the area of the rectangle at which it is being evaluated, provided the increments in u for the contours are the same for the whole curvilinear plot and similarly for v. The result of equation 49 then merely expresses the fractional number of curvilinear rectangles included in A_s.

This counting of the fractional number of curvilinear rectangles is a way of graphically evaluating waveform characteristics by the sequential turn on method since this method approximates $\vec{g}_A$ by $\vec{g}_{\hat{A}}$ which is either $\vec{0}$ or $\vec{g}_o$. This graphical method then consists of making a curvilinear plot on A with equal changes in u and equal changes in v to define curvilinear rectangles. If any field has reached a particular curvilinear rectangle at the time of interest, then that curvilinear rectangle is counted when determining the fractional number of curvilinear rectangles which are turned on so as to estimate the waveform at the time of interest by this crude method.

For purposes of calculating f_1 we have assumed a continuous distribution of $\vec{E}_s$ on S_s, turning on as a step function in an appropriate retarded-time manner. However a practical array is composed of numerous discrete pulsers connected together and arranged to approximate a continuous finite-size source surface. In such a case the TEM mode waveform $\alpha_o(t)$ will not rise to f_1 instantaneously but will require some time t_1 to do this. As

discussed in reference 3 this local turn on time for the array elements is typically composed of two parts. First there is the rise of the wave coming from the output switch(es) of each array module; this includes switch inductance, impedance the module has to drive at early times, etc. Second there is the time for the wave to extend over a plane at the output face of the module which involves the module size and geometry for wave guiding; this phenomenon is the same kind of effect on the individual module scale as occurs for the TEM mode turn on for the transmission line on a larger scale of dimensions. Note that the sequential turn on method for computing the TEM mode on the transmission line is best used for relative comparisons since it is not very accurate and the results depend in some cases on the position chosen for A. In like manner the turn on time for the local piece of the TEM mode turned on by each module depends on how far away the first signals from such a module are evaluated if a sequential turn on method is used; for such a method the turn on time for an individual module should be evaluated as close to the module as possible. Another approximate way to view the geometric part of the local module turn on is to imagine that conducting sheets on surfaces of constant u are placed between modules and extend from S_S to A_S; on surfaces of constant v one can imagine placing magnetic walls as well between modules. This defines many small transmission lines, one for each pulser module, extending between S_S and A_S. The rise of the TEM mode on each of these transmission lines is related to the cross section dimensions of the transmission line and how well the module is designed to launch a fast rising TEM wave on a transmission line of such cross section dimensions. Note that t_1 may vary over the various array modules (because of spacing etc.) and some effective value of t_1 may need to be estimated.

In any event we associate a time t_1 with the effective turn on of the individual modules. As shown in figure 2 this is the time required for the TEM waveform $\alpha_0(t)$ to rise to f_1, the initial TEM mode fraction associated with the entire pulser array idealized as S_S. Having f_1 and t_1 one figure of merit for the TEM waveform can be defined as

$$\tau_1 \equiv \frac{t_1}{f_1} \tag{50}$$

This is a time constant for the initial waveform rise if the waveform were a linear ramp for $0 < t < t_1$. As such $1/\tau_1$ is an indicator of the high frequency content of the TEM waveform. Thus small τ_1 is desired for arrays driving transmission lines, and as such can be considered a figure of merit. Note that if f_1^* is used instead of f_1 then we would also have

$$\tau_1^* \equiv \frac{t_1}{f_1^*} \tag{51}$$

Having considered figures of merit for the early rise portion of the TEM waveform let us go on to consider what might be termed the second portion of the rise of the waveform. Assume that the time t_p to the waveform peak is large compared to t_1 so that this portion of the waveform can be considered separately. For our present purpose then let the array be described by the continuous source field $\bar{E}_s$ on S_s as discussed previously. This simplifies matters by making $t_1 = 0$ and $\alpha_o(0+) = f_1$.

Then let us characterize the waveform as it rises from f_1 (perhaps not monotonically) toward 1.0 for the case that $\bar{E}_s$ is a step function. Define an effective time for this rise by

$$t_2' \equiv 2\int_o^{t_2} [f_2 - \alpha_o(t)]dt \tag{52}$$

where

$$f_1 < f_2 \leq 1$$
$$\alpha_o(t_2) = f_2 \tag{53}$$

The quantity f_2 is chosen for convenience to make comparisons of various waveforms. It might be .9 or so. If it can be made 1.0 with $\alpha_o(t)$ asymptotically approaching 1 fast enough that the integral converges then a good form for t_2' is

$$t_2' = 2\int_o^{\infty} [1 - \alpha_o(t)]dt \tag{54}$$

However, if there are convergence problems it may be necessary to choose $f_2 < 1$. In such a case it should be the same number for all arrays being compared, and of course it is required that $f_2 \geq f_1$ for all such arrays. Note that a real array gives a decaying waveform due to its finite capacitance so that $\alpha_o(t)$ may not reach 1 in a real case, but rather a peak f_p. In such a case it may be useful to set $f_2 \leq f_p$ as well as other choices such as in equation 54. In any event smaller t_2' gives a better waveform and so t_2' is another figure of merit.

Note the factor of 2 in the definition of t_2' is included to double the area of the difference of $\alpha_o(t)$ from unity. If $\alpha_o(t)$ were a linear ramp from f_1 to f_2 then $\alpha_o(t)$ would reach f_2 in a time $t_2'/(f_2 - f_1)$ giving a new time constant as

$$\tau_2 \equiv \frac{t_2'}{f_2 - f_1} \tag{55}$$

which for a linear ramp is the reciprocal of the slope. Thus $1/\tau_2$ is an indicator of the relative high frequency content of the waveform between f_1 and 1 (or f_2). Then τ_2 and t_2' are other figures of merit although perhaps not as important as τ_1 which gives the dominant high frequency content of the waveform. One would not want to decrease τ_2 at the expense of small f_1. Perhaps t_2' is then more important than τ_2. In any event τ_1 and τ_2 have roughly consistent definitions which become equivalent for the case of linear ramps. An alternate way of defining τ_2 is

$$\tau_2' \equiv \frac{t_2}{f_2 - f_1} \tag{56}$$

which reduces to τ_2 for a linear ramp with $t_1 = 0$.

One way of looking at the waveform $\alpha_o(t)$ for its early time characteristics is to consider it the sum of two waveforms. The first part is the waveform of amplitude f_1 rising in a time t_1. The second part is the waveform of amplitude $f_2 - f_1$ (or $1 - f_1$) rising in a time t_2 (or τ_2 or τ_2'). The high frequency content is governed by the first waveform, but as one goes down toward intermediate frequencies the second part of the waveform can still make a significant contribution.

A crude estimate for τ_2' (and thereby other variants of it) can be made using the sequential turn on method to approximate the waveform $\alpha_o(t)$ from equation 29. One replaces $\vec{g}_A$ by $\vec{g}_o$ or $\vec{0}$ in equation 29 and numerically approximates the integral. Since we are using $\vec{g}_o$ or $\vec{0}$ in the integral, then counting curvilinear rectangles that are turned on at time t and dividing by the total number of curvilinear rectangles gives an approximate value to $\alpha_o^*(t)$. As the size of the curvilinear rectangles tends to zero the answer is $\alpha_o^*(t)$. Again note that equal values of change in u and equal values of change in v are required over all of A if simple counting of curvilinear rectangles and dividing by the total is to apply. To determine whether or not a given curvilinear rectangle is turned on one has to calculate the time delay from the source array to say the center of each curvilinear square in $A - A_s$. In each case the array, if sloped, turns on at different times over S_s. Then the

geometrically closest position on the array to a curvilinear rectangle is not necessarily the array position to consider. One needs to find that position on the array which can first propagate a signal to the curvilinear rectangle in question. Having an approximation for $\alpha_o^*(t)$ we can then find

$$t_2'^* \equiv 2\int_o^{t_2^*} [f_2 - \alpha_2^*(t)]dt$$

$$\alpha_2^*(t_2^*) = f_2 \qquad (57)$$

$$\tau_2^* \equiv \frac{t_2'^*}{f_2 - f_1^*}$$

$$\tau_2'^* \equiv \frac{t_2^*}{f_2 - f_1^*}$$

After considering the early time figures of merit those for later times can be included. First the decay time constant τ_d is given from simple circuit concepts as

$$\tau_d = Z_c C_s \qquad (58)$$

where Z_c is the characteristic impedance of the transmission line given by

$$Z_c = f_g Z_o , \quad f_g = \frac{\Delta u}{\Delta v} \qquad (59)$$

where Δu is the change in the potential function between the plates and Δv is the change in the stream function on a path encircling the current in one plate (or several conductors depending on which currents one includes to define the impedance). The total capacitance of the array is C_s with the series-parallel connections of the individual module capacitances taken into account.

This decay constant fits into a late time waveform approximately as

$$\alpha_o(t) \approx e^{-t/\tau_d} \qquad (60)$$

for $t >> t_p$ (time of the peak). For this expression to be accurate one requires $\tau_d >> t_p$ so that the early time waveform distortion in the sense of deviation from the ideal waveform

$$\alpha_o(t)\Big|_{ideal} = e^{-t/\tau_d}u(t) \tag{61}$$

does not have a sufficient time integral to raise the amplitude of the waveform at late time in order to conserve the time integral of the waveform. Note that we have

$$\int_o^\infty \alpha_o(t)\,dt = \tau_d = Z_c C_s \tag{62}$$

independent of the early time effects. This merely expresses the fact that the complete time integral of a waveform is related to its low frequency asymptotic form, which in this case is given by the total charge (time integral of current) that the array delivers to the transmission line. Note then from equation 62 that τ_d has another interpretation relating to pulse width in the sense of complete time integral. One can compare this integral for τ_d to another one in equation 52 for t_2' for assumed step function excitation. To make some of the expressions more accurate then one would like $t_2'/2 << \tau_d$.

The characteristic impedance of the transmission line Z_c is used under the assumption that the transmission line is terminated in this impedance, at least at low frequencies. There is also a matter of consistency if more than one pulser array is used (such as in ATLAS I, designs 1 and 2). The definitions of Z_c and C_s must be consistent. Both should refer to the same combination of transmission lines and the product $Z_c C_s$ for a single transmission line (such as a conical wave launcher) should be the same for all TEM transmission lines that are combined to launch a TEM wave on a single transmission line, if this is done by separately launching portions of this wave over separate parts of the cross section of the single transmission line. Perhaps special low frequency matching networks could be used to allow one pulser to provide the low frequencies for radian wavelengths larger than the cross section dimensions of the single transmission line, but that is another problem.

This leaves one more figure of merit f_p, the peak value of $\alpha_o(t)$. To estimate this peak one can compare the early time calculations for $\alpha_o(t)$ using step function excitation on a continuous array as in equation 29 (or for $\alpha_o^*(t)$ using the sequential turn on method) to the late time form of $\alpha_o(t)$ including decay as in equation 60. Where the early and late time

approximations cross is one crude estimate for f_p. Perhaps a more accurate estimate could be made by taking the early time form of $\alpha_o(t)$ for step excitation and convoluting it with the derivative of the ideal late time waveform as in equation 61 giving

$$\alpha_o(t)\Big|_{\text{all time}} \simeq \alpha_o(t)\Big|_{\text{early time}} * \left[\delta(t) - \frac{1}{\tau_d} e^{-t/\tau_d} u(t)\right]$$

$$= \alpha_o(t)\Big|_{\text{early time}}$$

$$- \frac{u(t)}{\tau_d} \int_o^t \alpha_o(t - t')\Big|_{\text{early time}} e^{-t'/\tau_d} dt' \qquad (63)$$

Then f_p would be taken as the peak of this estimate. Note that equation 63 is not exact and only a reasonable approximation if $\tau_d >> t_p$ so that the low-frequency source impedance effects on the waveform are not very large in our estimate of the early time waveform.

Of course f_p (or peak field) is not necessarily the most important waveform parameter. Certainly if one looks at the Fourier transform of the waveform the low frequencies are dominated by τ_d and the high frequencies are dominated by τ_1 and more sophisticated details of the early rise. Both of these are scaled with the amplitude (in volts/m, amps/m, etc.) that goes in front of $\alpha_o(t)$ so that τ_d gives the waveform integral and τ_1 an initial slope. For intermediate frequencies more detailed waveform characteristics are important, but enter in a more complex manner. However, one might say sacrifice some on the magnitude of f_p while decreasing t_2' say, and not consider f_p as any absolute.

V. Summary

This note has considered some of the effects associated with launching TEM waves on cylindrical transmission lines or conical transmission lines with small cone angles between outermost portions of conductors. The wave is being launched by a finite size pulser array where the pulsers are assumed to be rather simple capacitive generators. Based on these considerations several figures of merit for the waveform can be defined, including ones associated with a fast initial rise, the subsequent rise toward the peak, the peak value, and the exponential decay. Some rough techniques for estimating some of these numbers are also discussed.

More detailed calculations of various boundary value problems are needed to better quantify the calculation of these waveforms and the associated figures of merit. Such calculations can even suggest more figures of merit to characterize significant features of such waveforms.

There are various questions about waveforms which these figures of merit do not address. These include details of the intermediate frequency characteristics of the waveforms, or the behavior of the Laplace transform of the waveforms in the complex frequency plane at roughly intermediate frequencies corresponding to possible natural frequencies of objects under test in a transmission line simulator. In other words it is still possible to have poor waveforms which have good figures of merit corresponding to the present list. These figures of merit correspond to some of the more apparent characteristics of pulser arrays. More subtle effects can enter from various aspects of the design of the individual modules and how the modules are electrically connected together to form an array.

References

1. Capt Carl E. Baum, Interaction Note 76, Electromagnetic Pulse Interaction Close to Nuclear Bursts and Associated EMP Environment Specification, July 1971.

2. Carl E. Baum, Interaction Note 88, On the Singularity Expansion Method for the Solution of Electromagnetic Interaction Problems, December 1971.

3. Carl E. Baum, Sensor and Simulation Note 143, General Principles for the Design of ATLAS I and II, Part I: ATLAS: Electromagnetic Design Considerations for Horizontal Version, January 1972.

4. Carl E. Baum, Sensor and Simulation Note 146, General Principles for the Design of ATLAS I and II, Part IV: Additional Considerations for the Design of Pulser Arrays, March 1972.

5. Robert E. Collin, Field Theory of Guided Waves, McGraw Hill, 1960, chapter 11.

6. Lt Carl E. Baum, Sensor and Simulation Note 21, Impedances and Field Distributions for Parallel Plate Transmission Line Simulators, June 1966.

7. Terry L. Brown and Kenneth D. Granzow, Sensor and Simulation Note 52, A Parameter Study of Two Parallel Plate Transmission Line Simulators of EMP Sensor and Simulation Note 21, April 1968.